

# Numerical study on Anderson transitions in three-dimensional disordered systems in random magnetic fields

Tohru Kawarabayashi\*

*Institute for Solid State Physics, University of Tokyo, Roppongi, Minato-ku, Tokyo 106, Japan*

Bernhard Kramer

*I. Institut für Theoretische Physik, Universität Hamburg, Jungiusstraße 9, D-20355 Hamburg, Germany*

Tomi Ohtsuki

*Department of Physics, Sophia University, Kioi-cho 7-1, Chiyoda-ku, Tokyo 102, Japan*

(October 9, 2018)

The Anderson transitions in a random magnetic field in three dimensions are investigated numerically. The critical behavior near the transition point is analyzed in detail by means of the transfer matrix method with high accuracy for systems both with and without an additional random scalar potential. We find the critical exponent  $\nu$  for the localization length to be  $1.45 \pm 0.09$  with a strong random scalar potential. Without it, the exponent is smaller but increases with the system sizes and extrapolates to the above value within the error bars. These results support the conventional classification of universality classes due to symmetry. Fractal dimensionality of the wave function at the critical point is also estimated by the equation-of-motion method.

71.30.+h, 71.23.-k, 72.15.Rn, 64.60.-i

## I. INTRODUCTION

Since the pioneering work by Anderson<sup>1</sup>, the metal-insulator transition driven by disorder, which is called the Anderson transition(AT), has attracted much attention for many years<sup>2-5</sup>. The critical behavior of the AT is conventionally classified, depending on the symmetry of hamiltonians, into three universality classes: the orthogonal, the unitary and the symplectic classes<sup>6</sup>. Systems invariant under spin rotation as well as time reversal form the orthogonal class. The unitary class is characterized by the absence of the time reversal symmetry. Systems invariant under time reversal but having no spin rotation symmetry belong to the symplectic class.

In the last decade, there has been considerable progress in the numerical study of the AT in three dimensions(3D) by the finite-size scaling analysis for quasi-1D systems<sup>7</sup>. In the early stage, it was not easy to confirm numerically for the 3D orthogonal class that the critical exponent is insensitive to the choice of the probability distribution of random potential<sup>8</sup>. This discrepancy in exponents for different distributions of random potential has been removed by improving the accuracy of numerical calculations<sup>9</sup> and by taking into account the corrections to scaling<sup>10</sup>. With such a high-accuracy analysis, it has been concluded that the critical exponent for the orthogonal system can be distinguished from that for the unitary system<sup>11</sup>. These recent developments confirm the universality of critical exponents as well as the validity of the conventional classification of universality classes in AT. It should be noted, however, that in most cases, such analyses have been restricted to the AT near the band center in the presence of a random scalar potential, where the scaling analysis works fairly well. In contrast, for the AT away from the band center, no systematic scaling behavior has been observed<sup>8,12</sup>.

The AT in a magnetic field has been studied extensively, mainly in connection with the quantum Hall effect<sup>13,14</sup>. Accordingly, in most cases, the magnetic field was assumed to be uniform in space and the disorder was introduced by a random scalar potential. On the other hand, in recent years, there has also been considerable interest in the transport properties of a system subject to a spatially random magnetic field. The random magnetic field introduces randomness as well as the absence of invariance under time reversal in a system. In fact, it has been shown<sup>15</sup> that in 3D the AT occurs in the presence of the random magnetic field and without a random scalar potential.

The AT in a random magnetic field is driven by the coherent scattering due to a fluctuating vector potential. A nontrivial feature of this coherent scattering by a fluctuating vector potential has been pointed out<sup>16</sup> in a theory of strongly correlated spin systems. Much work has also been done on transport properties in 2D in a random magnetic

---

\*Present Address: Faculty of Science, Toho University, Miyama 2-2-1, Funabashi, Chiba 274, Japan

field<sup>17</sup>, in particular in connection with the theory of the fractional quantum Hall effect<sup>18</sup> in a high magnetic field. It is thus an important issue to understand how the effect of coherent scattering in a strongly fluctuating random vector potential will show up in the AT.

The magnetic field breaks the time reversal symmetry and thus all systems in the magnetic field should belong to the unitary class. In fact, it has been demonstrated numerically in 3D<sup>20,22</sup> that in the presence of a random scalar potential, the critical exponent takes a universal value, irrespective of whether the magnetic field is uniform or random. The AT with a random potential and in a uniform magnetic field has been re-analyzed recently and the critical exponent for the localization length has been determined to be  $1.43 \pm 0.06$ <sup>11</sup>.

The AT, in 3D, in the presence of a random vector potential and without a random scalar potential, has also been investigated based on the finite-size scaling. The data suggested<sup>15</sup> that the mobility edge is very close to the band edge. The exponent for the localization length has been estimated to be  $\nu \approx 1$ <sup>15</sup> which is considerably smaller than that in the case with an additional random scalar potential and in a uniform magnetic field. This seemed to indicate that in 3D the AT driven solely by a random vector potential might exhibit critical behavior different from that observed in other unitary systems, for example systems having additional random scalar potential. Apparently, this questions the validity of the conventional classification of universality classes in AT. On the other hand, it should be recalled that the finite-size scaling analysis did not work for the AT near the effective band edge<sup>8,12</sup>. It is thus important to re-examine the applicability of the scaling ansatz to the AT driven solely by the random magnetic field in which the mobility edge lies quite close to the band edge.

In this paper, we report on a high-precision numerical finite-size scaling analysis for the AT in the random magnetic field. In order to clarify the origin of the above mentioned discrepancy between the critical exponent of the AT far away from the band center induced solely by randomness in a vector potential and the exponent obtained for other unitary systems, we have considered systems both with and without an additional random potential. We also evaluate the fractal dimension of the wave functions at the critical point based on the equation-of-motion method.

The paper is organized as follows. In the next section, the hamiltonian which we adopt is introduced. The finite-size scaling study on the critical phenomena is presented in section 3. In section 4, the fractal dimensionality of the wave function is discussed by means of the equation-of-motion method. Section 5 is devoted to summary and discussion.

## II. MODEL

The model is defined by the Hamiltonian<sup>15</sup>

$$H = V \sum_{\langle i,j \rangle} \exp(i\theta_{i,j}) C_i^\dagger C_j + \sum_i \varepsilon_i C_i^\dagger C_i, \quad (1)$$

where  $C_i^\dagger (C_i)$  denotes the creation(annihilation) operator of an electron at the site  $i$  of a 3D cubic lattice. Energies  $\{\varepsilon_i\}$  denote the random scalar potential distributed independently and uniformly in the range  $[-W/2, W/2]$ . The Peierls phase factors  $\exp(i\theta_{i,j})$  describe a random vector potential or magnetic field. We confine ourselves to phases  $\{\theta_{i,j}\}$  which are distributed independently and uniformly in  $[-\pi, \pi]$ . The hopping amplitude  $t$  is assumed to be the energy unit,  $V = 1$ . The phases  $\{\theta_{i,j}\}$  are related to the magnetic flux, for example, as

$$\theta_{i,i+\hat{x}} + \theta_{i+\hat{x},i+\hat{x}+\hat{y}} + \theta_{i+\hat{x}+\hat{y},i+\hat{y}} + \theta_{i+\hat{y},i} = -2\pi\phi_i/\phi_0, \quad (2)$$

where  $\phi_i$  and  $\phi_0 = hc/|e|$  denote the magnetic flux through the plaquette  $(i, i + \hat{x}, i + \hat{x} + \hat{y}, i + \hat{y})$  and the unit flux, respectively. Here  $\hat{x}(\hat{y})$  stands for the unit vector in the  $x(y)$ -direction. Note that in the present system, the condition that the magnetic flux through a closed surface is zero is satisfied.

## III. FINITE-SIZE SCALING STUDY

We consider quasi-1D systems with cross section  $M \times M$ <sup>7,9</sup>. The Schrödinger equation  $H\psi = E\psi$  in such a bar-shaped system can be rewritten using transfer matrices  $T_n(2M^2 \times 2M^2)$

$$\begin{pmatrix} \psi_{n+1} \\ \psi_n \end{pmatrix} = T_n \begin{pmatrix} \psi_n \\ \psi_{n-1} \end{pmatrix}, \quad T_n = \begin{pmatrix} E - H_n & -I \\ I & 0 \end{pmatrix} \quad (3)$$

( $n = 1, 2, \dots$ ) where  $\psi_n$  and  $H_n$  denote the set of coefficients of the state  $\psi$  and the Hamiltonian of the  $n$ -th slice, respectively. The identity matrix is denoted by  $I$ . The off-diagonal parts of the transfer matrix  $T_n$  can be expressed

by the identity matrix because the phases in the transfer-direction can be removed by a gauge transformation<sup>15</sup>. The logarithms of the eigenvalues of the limiting matrix  $T$

$$T \equiv \lim_{n \rightarrow \infty} [(\prod_{i=1}^n T_i)^\dagger (\prod_{i=1}^n T_i)]^{1/2n} \quad (4)$$

are called the Lyapunov exponents. The smallest Lyapunov exponent  $\lambda_M$  along the bar is estimated by a technique which uses the product of these transfer matrices<sup>5,7</sup>. The relative accuracies for the smallest Lyapunov exponents achieved here is 0.2% for  $M \leq 10$  and 0.25%  $\sim$  0.3% for  $M = 12$ . The localization length  $\xi_M$  along the bar is given by the inverse of the smallest Lyapunov exponent,  $\xi_M = 1/\lambda_M$ .

The assumption of one-parameter scaling for the renormalized localization length  $\Lambda_M \equiv \xi_M/M$  implies

$$\Lambda_M = f(\xi/M), \quad (5)$$

where  $\xi = \xi(E, W)$  is the relevant length scale in the limit  $M \rightarrow \infty$ <sup>7</sup>. Near the mobility edge  $E_c(W)$ ,  $\xi$  diverges with an exponent  $\nu$  as  $\xi \sim x^{-\nu}$  with  $x = (E - E_c)/E_c$ . If the transition is driven by the disorder  $W$  at a constant energy,  $x = (W_c - W)/W_c$ . At the mobility edge,  $\Lambda_M$  becomes scale-invariant. The quantity  $\Lambda_M$  is a smooth function of  $E$  and  $W$ , and we can expand it as a function of  $x$  as

$$\Lambda_M = \Lambda_c + \sum_{n=1}^{\infty} A_n (M^{1/\nu} x)^n. \quad (6)$$

By fitting our data to the above function, we can determine the critical exponent  $\nu$  and the mobility edge accurately. In practice, we truncated the series (6) at the third order ( $n = 3$ ) and used the standard  $\chi^2$ -fitting procedure<sup>23</sup>. The error bars are estimated by using the Hessian matrix and the confidence interval is chosen to be 95.4%.

For the transition at the band center in the presence of a strong random scalar potential, a clear scaling has been observed for presently achievable sizes,  $6 \leq M \leq 12$ . In fact, all the data (84 points) for  $M = 6, 8, 10$ , and 12 in the range  $17.8 \leq W \leq 19.8$  can be successfully fitted by the fitting function (6) up to the 3rd order, which has six fitting parameters including the critical point and the critical exponent. We have estimated the critical disorder and the exponent  $\nu$  to be  $W_c = 18.80 \pm 0.04$  and  $\nu = 1.45 \pm 0.09$ <sup>24</sup>. The renormalized localization length  $\Lambda_c$  at the critical point is  $0.558 \pm 0.003$ . The error bars of these estimations are at least a factor of 3 smaller than those of the previous estimates<sup>20</sup>.

In contrast, in the absence of the random scalar potential ( $W = 0$ ) or in the presence of an additional weak random scalar potential ( $W = 1$ ), for which the critical point lies near the band edge, we have found<sup>24</sup> that the correction to scaling is not negligible. Near the band edge, the density of states changes rapidly as a function of energy. We have thus performed high-accuracy transfer matrix calculations for narrower energy range  $|E - E_c| \leq 0.025$  around the critical point for  $W = 0$  and  $W = 1$ <sup>24</sup>. In both cases ( $W = 0$  and  $W = 1$ ), we have found that the estimation of the critical exponent tends to increase with the system-sizes. In order to extrapolate the critical exponent for  $W = 0$ , we have made calculations for larger system sizes  $M = 14$  and  $M = 16$ . Here we show, in Table I, the summary of the results for  $W = 0$  obtained by the fittings with different sizes up to  $M = 16$ . The relative accuracy in  $\xi_M^{-1}$  achieved for  $M = 14$  and  $M = 16$  is 1% for each sample and 7 and 5 realizations of random phases are considered, respectively. The scaling regime is assumed to be  $[4.39, 4.44]$  as in ref. 24. It is clear that the critical point exists around  $E_c \approx 4.41$  (see figure 1). In Table 1, we can see that the exponent  $\nu$  tends to increase with the system-sizes and is likely to saturate around  $\nu \sim 1.48$ . Within the error bars, estimated values of  $\nu$  for  $M \geq 12$  are consistent with  $1.45 \pm 0.09$  obtained for the band center as well as  $1.43 \pm 0.06$  estimated in the uniform magnetic field<sup>11</sup>. No evidence has been found for  $\nu \approx 1$  which was suggested by calculations with low accuracy<sup>15</sup>. The present results support the universality of the critical exponent in the unitary systems. The positions of the critical points and the values of  $\Lambda_c$  estimated with different combinations of system-sizes are fluctuating for  $M \geq 12$  (Table I). The value of  $\Lambda_c = 0.558 \pm 0.003$  at the band center seems to lie inside the range of this fluctuation. Conventionally, the value of  $\Lambda_c$  is also expected to be universal in unitary systems. Our results obtained here seem to be consistent with this universality of  $\Lambda_c$ .

The mobility edge trajectory in the presence of the random magnetic field is shown in figure 2. Each critical point (mobility edge) is estimated based on numerical data by the transfer matrix method with  $M = 6 \sim 10$ . It should be noted that there exist extended states for energies larger than the critical energy  $E_c \approx 4.41$  for  $W = 0$ . This type of reentrant phenomena in the energy-disorder plane has been commonly observed for systems with the uniform distribution of random scalar potential<sup>26,27</sup>. It is interpreted<sup>26</sup> that the enhancement of extended states for a weak additional random scalar potential is due to the enhancement of density of states at that energy regime.

#### IV. EQUATION-OF-MOTION METHOD

We now turn our attention to the properties of wave function just at the AT in random magnetic fields. It is well known that at the AT, the wave function shows multifractal structure<sup>28</sup> which leads to the scale invariant behavior of conductance distributions<sup>29,30,11</sup> and the energy level statistics.<sup>31–38</sup>

The direct way to investigate the wave functions is to diagonalize the Hamiltonian. This, however, is numerically very intensive. Instead, we calculate here the time evolution of wave packets to extract the information of fractal dimension. We first prepare the initial wave packet  $|0\rangle$  close to AT by diagonalizing a small cluster located at the center of the system. The time evolution of the state at time  $t$  is then obtained by

$$|t + \Delta t\rangle = U(\Delta t)|t\rangle$$

where  $U(\Delta t)$  is the time evolution operator. In order to perform effectively the numerical calculation, we approximate  $U(\Delta t)$  by the products of exponential operators as

$$U(\Delta t) = e^{-iH\Delta t/\hbar} = U_2(p\Delta t)U_2((1-2p)\Delta t)U_2(p\Delta t) + O(\Delta t^5) \quad (7)$$

with  $p = (2 - 2^{1/3})^{-1}$  and

$$U_2(\Delta t) \equiv e^{-iH_1\Delta t/2\hbar} \dots e^{-iH_{q-1}\Delta t/2\hbar} e^{-iH_q\Delta t/\hbar} e^{-iH_{q-1}\Delta t/2\hbar} \dots e^{-iH_1\Delta t/2\hbar}, \quad (8)$$

where  $H_1, \dots, H_q$  are decomposition of the original Hamiltonian  $H = \sum_i H_i$  which are simple enough to diagonalize analytically.<sup>39</sup>

The square displacement of the wave packets is defined by

$$r^2(t) = \langle t | r^2 | t \rangle.$$

In metallic phase,  $r^2(t)$  is proportional to  $Dt$  where  $D$  is the diffusion coefficient. In the insulating phase, it saturates to the square of localization length,  $\xi^2$ . At AT, the anomalous diffusion<sup>41,42</sup>

$$r^2(t) \sim t^{2/d} = t^{2/3}$$

is expected. The fractal dimension  $D_2$  is estimated from the autocorrelation function

$$C(t) = \frac{1}{t} \int_0^t dt' |\langle t' | 0 \rangle|^2$$

where  $C(t)$  is expected to decay as<sup>43</sup>

$$C(t) \sim t^{-D_2/d}.$$

In Fig. 3, we show the results of  $C(t)$  for the transition at the center of the band in the presence of a strong random scalar potential ( $W = 18.8V$ ). By diagonalizing a small cluster of  $7 \times 7 \times 7$  located at the the center of the system, we follow the time evolution of wave packets in  $101 \times 101 \times 101$  systems. Geometric average of  $C(t)$  over 10 random field and potential configurations are performed. By fitting the data for  $t > 40\hbar/V$ , the fractal dimensionality  $D_2$  is estimated to be

$$D_2 = 1.52 \pm 0.18$$

considerably smaller than the space dimension  $d = 3$ . The above value is consistent with the estimate of 3D system at AT in a strong uniform magnetic field.<sup>42,44</sup>

#### V. DISCUSSIONS

In summary, we have investigated in detail the AT in a random magnetic field based on the transfer matrix method with considerably high accuracy. In particular, whether or not the AT driven solely by the random vector potential ( $W = 0$ ) exhibits different critical behavior from other unitary systems has been discussed. In order to clarify the above point, we have performed the scaling analysis for the three critical points, namely  $E = 0$ ,  $W = 0$ , and  $W = 1$  (figure 2). For the transition at the band center ( $E = 0$ ) in the presence of a strong additional random potential, a

clear scaling behavior has been observed and the exponent  $\nu$  has been estimated to be  $1.45 \pm 0.09$ . This coincides with the value obtained for a unitary system in a uniform magnetic field<sup>11</sup>. It has been found, on the other hand, that the correction to scaling is not negligible in the presently achievable sizes for the transitions near the band edge ( $W = 1$  and  $W = 0$ ). The exponents estimated for  $W = 0$  by larger system sizes are consistent with those obtained for other unitary systems within the error bars. From the size dependence of  $\nu$ , in contrast to the suggestion in ref.15, no evidence has been found for  $\nu \approx 1$ . These results indicate the universality of  $\nu$  in the unitary class and hence support the conventional classification of the AT by universality classes due to symmetry.

The mobility edge trajectory has been also obtained in the presence of the random magnetic field. Its qualitative shape turns out to be similar to those obtained for other systems with the uniform distribution of random scalar potential.

We have also studied the diffusion of electrons at the AT in the presence of a random magnetic field. By solving the time-dependent Schrödinger equation numerically, we examine the time evolution of wave packets at the AT. From the asymptotic behavior of the autocorrelation function, we have extracted the fractal dimensionality of the critical wave function at the band center.

## ACKNOWLEDGMENTS

The authors thank M. Batsch, A. MacKinnon, I. Zharekeshev and K. Slevin for valuable discussions. The numerical calculations were performed on a FACOM VPP500 of Institute for Solid State Physics, University of Tokyo and in computer facilities of I. Institut für Theoretische Physik, Universität Hamburg. This work was supported in part by the EU-project FHRX-CT96-0042 and by the Deutsche Forschungsgemeinschaft via Project Kr627/10 and the Graduiertenkolleg "Nanostrukturierte Festkörper". One of the authors (T.K.) thanks Alexander von Humboldt Foundation for financial support during his stay at University of Hamburg where the present work has been started.

- 
- <sup>1</sup> P.W. Anderson, Phys. Rev. **109** (1958) 1492
  - <sup>2</sup> F. Wegner, Z. Phys. **B25** (1976) 327; **B35** (1979) 207
  - <sup>3</sup> S. Hikami, Phys. Rev. **B24** (1981) 2671
  - <sup>4</sup> P.A. Lee and T.V. Ramakrishnan, Rev. Mod. Phys. **57** (1985) 287
  - <sup>5</sup> B. Kramer and A. MacKinnon, Rep. Prog. Phys. **56** (1993) 1469
  - <sup>6</sup> F.J. Dyson, J. Math. Phys. **3**, (1962) 140; **3** (1962) 157; **3** (1962) 166
  - <sup>7</sup> A. MacKinnon and B. Kramer, Phys. Rev. Lett. **47** (1981) 1546; Z. Phys. B **53** (1983) 1
  - <sup>8</sup> B. Kramer, K. Broderix, A. MacKinnon and M. Schreiber, Physica A **167** (1990) 163
  - <sup>9</sup> A. MacKinnon, J. Phys.: Condens. Matter **6** (1994) 2511
  - <sup>10</sup> K. Slevin and T. Ohtsuki, Phys. Rev. Lett. **82** (1999) 382
  - <sup>11</sup> K. Slevin and T. Ohtsuki, Phys. Rev. Lett. **78** (1997) 4083
  - <sup>12</sup> M. Schreiber and B. Kramer, in *Anderson Transition* edited by T.Ando and H.Fukuyama, 92 (Springer-Verlag 1988).
  - <sup>13</sup> *Introduction to the Theory of the Integer Quantum Hall Effect*, J. Hajdu *et al.*, (VCH, 1994)
  - <sup>14</sup> B. Huckestein, Rev. Mod. Phys. **67** (1994) 357
  - <sup>15</sup> T. Ohtsuki, Y.Ono and B. Kramer, J. Phys. Soc. Jpn. **63** (1994) 685
  - <sup>16</sup> B. Altshuler and L.B. Ioffe, Phys. Rev. Lett. **69** (1992) 2979
  - <sup>17</sup> A. Furusaki, Phys. Rev. Lett. **82** (1999) 604.
  - <sup>18</sup> B.I. Halperin, P.A. Lee, and N. Read, Phys. Rev. **B47** (1993) 7312
  - <sup>19</sup> T. Ohtsuki, B. Kramer and Y. Ono, J. Phys. Soc. Jpn. **62** (1993) 224
  - <sup>20</sup> M. Henneke, B. Kramer and T. Ohtsuki, Euro. Phys. Lett. **27** (1994) 389
  - <sup>21</sup> J.T. Chalker and A. Dohmen, Phys. Rev. Lett. **75** (1995) 4496
  - <sup>22</sup> B. Kramer, T. Ohtsuki and M. Henneke, in *Quantum Dynamics of Submicron Structures*, edited by H.A. Cerdeira *et al.*, 21 (Kluwer Academic Publishers, 1995)
  - <sup>23</sup> W.H. Press *et al.*, Numerical Recipes (Cambridge University Press, 1986)
  - <sup>24</sup> T. Kawarabayashi, B. Kramer, and T.Ohtsuki, Phys. Rev. **B57** (1998) 11842
  - <sup>25</sup> T. Kawarabayashi, B. Kramer, and T. Ohtsuki, J. Phys. : Condens. Matter **10** (1998) 11547
  - <sup>26</sup> B. Bulka, M. Schreiber, and B. Kramer, Z. Phys. **B66** (1987) 21
  - <sup>27</sup> T. Dröse, M. Batsch, I. Zharekeshev, and B. Kramer, Phys. Rev. **B57**(1998) 37

- <sup>28</sup> H. Aoki, J. Phys. C **16** (1983) L205; C.M. Soukoulis and E.N. Economou, Phys. Rev. Lett. **52** (1984) 565; M. Schreiber, Phys. Rev. B **31** (1985) 6146; Y. Ono, B. Kramer and T. Ohtsuki, J. Phys. Soc. Jpn. **58** (1989) 1705; M. Schreiber and H. Grussbach, Phys. Rev. Lett. **67** (1991) 607; B. Pook and M. Janssen, Z. Phys. B **82** (1991) 295
- <sup>29</sup> B. Shapiro, Phys. Rev. Lett. **65** (1990) 1510; A. Cohen and B. Shapiro, Int. J. Mod. Phys. **B6** (1992) 1243
- <sup>30</sup> P. Markos and B. Kramer, Phil. Mag. **B68** (1993) 357
- <sup>31</sup> B.I. Shklovskii, B. Shapiro, B.R. Sears, P. Lambrianides and H.B. Shore, Phys. Rev. **B47** (1993) 11487
- <sup>32</sup> Y. Ono and T. Ohtsuki, J. Phys. Soc. Jpn. **62** (1993) 3813
- <sup>33</sup> E. Hofstetter and M. Schreiber, Phys. Rev. **B48** (1993) 16979; **B49** (1994) 14726
- <sup>34</sup> S.N. Evangelou, Phys. Rev. **B49** (1994) 16805
- <sup>35</sup> I. Kh. Zharekeshev and B. Kramer, Jpn. J. Appl. Phys. **34** (1995) 4361; Phys. Rev. **B51** (1995) 17239; Phys. Rev. Lett **79** (1997) 717
- <sup>36</sup> M. Batsch, L. Schweitzer, I. Kh. Zharekeshev and B. Kramer, Phys. Rev. Lett. **77** (1996) 1552
- <sup>37</sup> L. Schweitzer and I. Kh. Zharekeshev, J. Phys.: Condens. Matter **9** (1997) L377
- <sup>38</sup> T. Kawarabayashi, T. Ohtsuki, K. Slevin and Y. Ono, Phys. Rev. Lett. **77** (1996) 3593
- <sup>39</sup> M. Suzuki, Phys. Lett. **A146** (1990) 319; J. Math. Phys. **32** (1991) 400; J. Phys. Soc. Jpn. **61** (1992) 3015; Commun. Math. Phys. **163** (1994) 491
- <sup>40</sup> T. Kawarabayashi and T. Ohtsuki, Phys. Rev. **B51** (1995) 10897
- <sup>41</sup> B. Shapiro: in *Percolation structures and Process*, ed. G. Deutscher *et al.* Ann. Isr. Phys. Soc. (1983) 367
- <sup>42</sup> T. Ohtsuki and T. Kawarabayashi, J. Phys. Soc. Jpn. **66** (1997) 314
- <sup>43</sup> T. Brandes, B. Huckestein, and L. Schweitzer, Ann. Physik **5** (1996) 633
- <sup>44</sup> B. Huckestein and R. Klesse, Phil. Mag. **B77** (1998) 1181

$(M_1, M_2)$	$\Lambda_c$	$\nu$	$E_c$	$N$	$\chi_{min}^2$
(6,8)	$0.514 \pm 0.005$	$1.05 \pm 0.07$	$4.414 \pm 0.001$	42	$\sim 84.3$
(8,10)	$0.516 \pm 0.007$	$1.26 \pm 0.09$	$4.414 \pm 0.001$	42	$\sim 30.0$
(10,12)	$0.51 \pm 0.01$	$1.32 \pm 0.12$	$4.414 \pm 0.001$	42	$\sim 15.9$
(12,14)	$0.56 \pm 0.02$	$1.49 \pm 0.16$	$4.409 \pm 0.002$	42	$\sim 18.7$
(14,16)	$0.48 \pm 0.02$	$1.475 \pm 0.19$	$4.417 \pm 0.002$	42	$\sim 32.4$
(12,16)	$0.53 \pm 0.01$	$1.46 \pm 0.09$	$4.413 \pm 0.001$	42	$\sim 18.6$

TABLE I. Results for  $\Lambda_c$ ,  $\nu$ , and  $E_c$  by the fits using the data for two system-sizes  $M_1$  and  $M_2$  for  $W = 0$ . Here  $N$  stands for the number of data used for the fit, and  $\chi_{min}^2$  denotes the minimum value of  $\chi^2$  obtained by the fit.

$E$	$\Lambda_6$	$\Lambda_8$	$\Lambda_{10}$	$\Lambda_{12}$	$\Lambda_{14}$	$\Lambda_{16}$
4.3900	$0.650 \pm 0.001$	$0.696 \pm 0.001$	$0.736 \pm 0.001$	$0.777 \pm 0.002$	$0.808 \pm 0.002$	$0.843 \pm 0.003$
4.3925	$0.634 \pm 0.001$	$0.675 \pm 0.001$	$0.709 \pm 0.001$	$0.745 \pm 0.002$	$0.768 \pm 0.003$	$0.799 \pm 0.002$
4.3950	$0.620 \pm 0.001$	$0.654 \pm 0.001$	$0.686 \pm 0.001$	$0.713 \pm 0.002$	$0.729 \pm 0.002$	$0.765 \pm 0.003$
4.3975	$0.605 \pm 0.001$	$0.634 \pm 0.001$	$0.658 \pm 0.001$	$0.683 \pm 0.002$	$0.696 \pm 0.002$	$0.721 \pm 0.004$
4.4000	$0.588 \pm 0.001$	$0.614 \pm 0.001$	$0.636 \pm 0.001$	$0.654 \pm 0.002$	$0.664 \pm 0.002$	$0.688 \pm 0.002$
4.4025	$0.574 \pm 0.001$	$0.595 \pm 0.001$	$0.609 \pm 0.001$	$0.627 \pm 0.002$	$0.635 \pm 0.002$	$0.652 \pm 0.005$
4.4050	$0.561 \pm 0.001$	$0.575 \pm 0.001$	$0.588 \pm 0.001$	$0.600 \pm 0.002$	$0.603 \pm 0.001$	$0.613 \pm 0.004$
4.4075	$0.546 \pm 0.001$	$0.557 \pm 0.001$	$0.565 \pm 0.001$	$0.575 \pm 0.001$	$0.573 \pm 0.002$	$0.587 \pm 0.001$
4.4100	$0.530 \pm 0.001$	$0.540 \pm 0.001$	$0.546 \pm 0.001$	$0.549 \pm 0.001$	$0.547 \pm 0.002$	$0.554 \pm 0.003$
4.4125	$0.517 \pm 0.001$	$0.522 \pm 0.001$	$0.524 \pm 0.001$	$0.526 \pm 0.001$	$0.522 \pm 0.002$	$0.529 \pm 0.002$
4.4150	$0.506 \pm 0.001$	$0.505 \pm 0.001$	$0.505 \pm 0.001$	$0.502 \pm 0.001$	$0.498 \pm 0.002$	$0.497 \pm 0.002$
4.4175	$0.494 \pm 0.001$	$0.492 \pm 0.001$	$0.484 \pm 0.001$	$0.481 \pm 0.001$	$0.474 \pm 0.002$	$0.473 \pm 0.001$
4.4200	$0.483 \pm 0.001$	$0.474 \pm 0.001$	$0.468 \pm 0.001$	$0.461 \pm 0.001$	$0.453 \pm 0.001$	$0.452 \pm 0.002$
4.4225	$0.472 \pm 0.001$	$0.459 \pm 0.001$	$0.450 \pm 0.001$	$0.443 \pm 0.001$	$0.432 \pm 0.001$	$0.424 \pm 0.002$
4.4250	$0.457 \pm 0.001$	$0.445 \pm 0.001$	$0.433 \pm 0.001$	$0.423 \pm 0.001$	$0.411 \pm 0.001$	$0.404 \pm 0.002$
4.4275	$0.448 \pm 0.001$	$0.431 \pm 0.001$	$0.417 \pm 0.001$	$0.405 \pm 0.001$	$0.393 \pm 0.002$	$0.383 \pm 0.001$
4.4300	$0.438 \pm 0.001$	$0.418 \pm 0.001$	$0.401 \pm 0.001$	$0.387 \pm 0.001$	$0.373 \pm 0.001$	$0.364 \pm 0.001$
4.4325	$0.428 \pm 0.001$	$0.405 \pm 0.001$	$0.387 \pm 0.001$	$0.371 \pm 0.001$	$0.355 \pm 0.001$	$0.345 \pm 0.001$
4.4350	$0.420 \pm 0.001$	$0.391 \pm 0.001$	$0.374 \pm 0.001$	$0.356 \pm 0.001$	$0.339 \pm 0.001$	$0.328 \pm 0.001$
4.4375	$0.409 \pm 0.001$	$0.382 \pm 0.001$	$0.359 \pm 0.001$	$0.342 \pm 0.001$	$0.323 \pm 0.001$	$0.313 \pm 0.001$
4.4400	$0.402 \pm 0.001$	$0.369 \pm 0.001$	$0.347 \pm 0.001$	$0.328 \pm 0.001$	$0.308 \pm 0.002$	$0.298 \pm 0.001$

TABLE II. List of numerical data of  $\Lambda_M$  presented in figure 1 for  $W = 0$ .

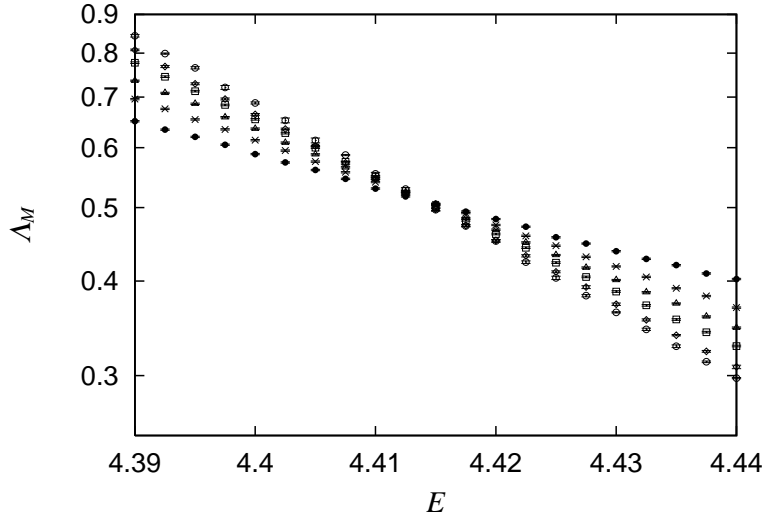


FIG. 1. Renormalized localization lengths for  $W = 0$  are presented in log-scale as a function of energy. The dots, the crosses, the triangles, the squares, the diamonds, the circles correspond to  $M = 6, 8, 10, 12, 14$ , and  $16$ , respectively.

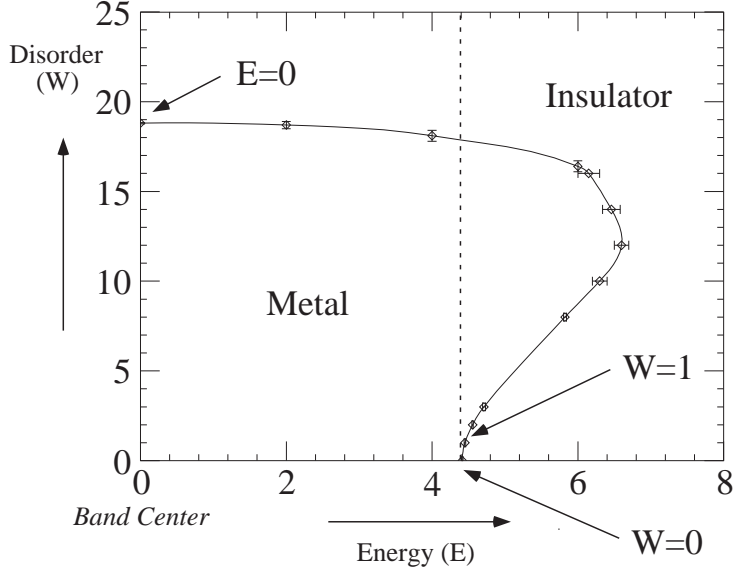


FIG. 2. Mobility edge trajectory for the 3D system in the random magnetic field. The re-entrant phenomenon is clearly seen.



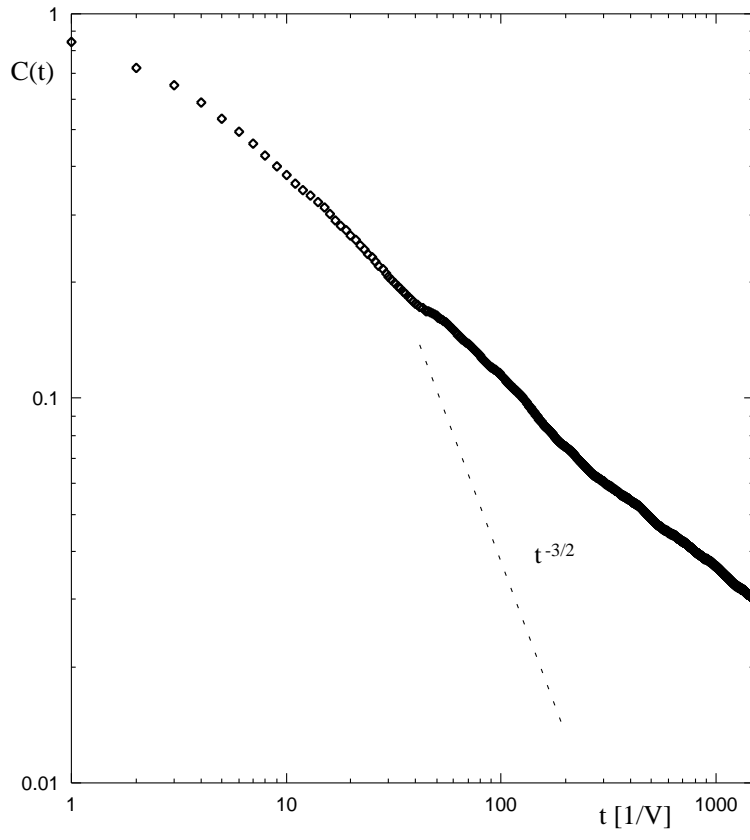


FIG. 3. The autocorrelation function  $C(t)$  as a function of  $t$ . Dashed lines represent the decay  $\propto t^{-3/2}$ .